

Article

Multilayer Nanoimprinting to Create Hierarchical Stamp Masters for Nanoimprinting of Optical Micro- and Nanostructures

Amiya R. Moharana, Helene M. Außerhuber, Tina Mitteramskogler , Michael J. Haslinger and Michael M. Mühlberger * 

PROFACTOR GmbH, Im Stadtgut A2, 4407 Steyr-Gleink, Austria; amiya.moharana@profactor.at (A.R.M.); helene.ausserhuber@profactor.at (H.M.A.); tina.mitteramskogler@profactor.at (T.M.); michael.haslinger@profactor.at (M.J.H.)

* Correspondence: michael.muehlberger@profactor.at

Received: 28 February 2020; Accepted: 17 March 2020; Published: 24 March 2020



Abstract: Nanoimprinting is a well-established replication technology for optical elements, with the capability to replicate highly complex micro- and nanostructures. One of the main challenges, however, is the generation of the master structures necessary for stamp fabrication. We used UV-based Nanoimprint Lithography to prepare hierarchical master structures. To realize structures with two different length scales, conventional nanoimprinting of larger structures and conformal reversal nanoimprinting to print smaller structures on top of the larger structures was performed. Liquid transfer imprint lithography proved to be well suited for this purpose. We used the sample prepared in such a way as a master for further nanoimprinting, where the hierarchical structures can then be imprinted in one single nanoimprinting step. As an example, we presented a diffusor structure with a diffraction-grating structure on top.

Keywords: Nanoimprint lithography; UV-NIL; reversal NIL; liquid transfer imprint lithography; hierarchical structures; optical micro- and nanostructures

1. Introduction

UV-based Nanoimprint Lithography [1,2] is a method to replicate nanostructures on a large area, and is commonly used for the fabrication of microlenses [3–5], wafer-level cameras [6,7] and diffractive optical elements [8–10]. The basic process flow is the following: a nanostructured stamp is pressed into a liquid, UV-curable material on a substrate. While the stamp is in contact with the polymer, the material is cured by UV-irradiation and then the stamp is removed, resulting in a nanostructured crosslinked polymer on the substrate. Typically, and for cost-of-ownership considerations, the stamp itself is a copy from a master structure, which can be prepared by many different types of fabrication methods, for example, electron beam lithography [11,12], ion beam lithography [13], x-ray lithography [14], diamond turning [10,15] and even by copying from natural structures [16]. For many applications, it is interesting to investigate nanostructures on top of larger microstructures: so-called ‘hierarchical structures’. Such structures often appear in nature (e.g., lotus flower leaves [17] or gecko feet [18,19]), but can also be interesting for other applications like grating couplers on waveguides (e.g., [20]), energy applications [21], or sensors [22]). Nanoimprinting is ideally suited to replicate complex structures in a single process step. In most cases it is, however, non-trivial to fabricate the complex master structure, which is then used for stamp fabrication. We investigated the combination of two nanoimprint steps to create such masters with hierarchical structures.

2. Materials and Methods

As nanoimprint materials, we focused, in this work, on UV-curable hybrid polymers, so-called ‘Ormocers’. They are commercially available and are designed for use in optical applications [23].

Usually, in nanoimprint lithography, it is the substrate which is coated with the UV-curable imprint polymer, e.g., by spin coating, droplet dispensing or inkjet printing. However, for certain applications, it can be advantageous to coat the stamp rather than the substrate, which is then called ‘reversal NIL’ [24]. This procedure is especially advantageous if NIL has to be performed on top of existing micro- or nanostructures while preserving the topography. It is usually not possible to apply a homogeneous coating directly on top of already existing micro- or nanostructures without filling up the gap between these structures or changing their geometry. However, reversal NIL is often challenging since the Nanoimprint stamps are designed to exhibit anti-sticking properties, which makes good wetting - and therefore homogeneous coating of the stamp – difficult, or leads to spontaneous dewetting. This puts limitations on the type of materials that can be used as well as on the type of stamps.

A variant of reversal NIL, so-called liquid-transfer imprint lithography (LTIL) [25], is a possible solution for this problem. The basic principle of LTIL is that, initially, a flat substrate is spin coated with the UV-curable resin. This so-called donor wafer is a material that can be spin-coated nicely. It is used to prepare a thin and well defined nanoimprint material layer on a substrate. Next, a flexible stamp is brought into contact with the resin layer on the donor wafer, and this stamp is then peeled off from the donor wafer in a well-controlled way. A thin, homogeneous layer of liquid UV-curable resin stays on the stamp, which is then transferred to the target substrate, where the UV-NIL process is finished by curing the resin by UV radiation and the subsequent demolding step.

This LTIL process can be used to nanoimprint a structure on an already prestructured substrate to combine different structures and functionalities [26–28]. In our work, we combined the optical effects of a line and space diffraction grating with that of a diffusor in order to create a sample with such a hierarchical pattern, which we then used as a new master for further stamp fabrication and imprinting, improving the facilitation of the overall process in the end. The diffusor and grating pattern was chosen to demonstrate the technology and has no specific application in the context of this work.

In the following paragraphs we describe the way in which we prepared our prestructured substrates, how we perform the LTIL nanoimprinting on top of the prestructured substrate, and how we used the result of this process as a master for working stamp fabrication and single-step imprinting of hierarchical structures.

As the material for our prestructured substrates, we chose OrmoComp [29] on a standard PVC foil. The 100- μm -thick PVC foils were used as received, without any further treatment. OrmoComp has good adhesion to PVC and excellent optical and nanoimprint properties. We used a standard nanoimprint process to pattern the OrmoComp and create an OrmoComp diffusor substrate. The stamps for this nanoimprint process were prepared by casting Polydimethylsiloxane (PDMS, Sylgard 184, 1:10 mixing ratio, 40 °C temperature, 23 h curing time) on a commercial diffusor foil. The imprint material was droplet dispensed onto the PVC substrate. UV curing was accomplished using an in-house built high-power UV-LED light source with a wavelength of 365 nm. For the imprinting, no pressure was applied. A photograph and an AFM image are shown in Figure 1. The typical peak to valley height is around 2.5 μm .

On top of the OrmoComp diffusor substrate, we performed the LTIL nanoimprint process. The stamps for this process were also made from PDMS (Sylgard 184, same procedure as for the diffusor PDMS stamp) and copied from a line and space quartz master (fabricated by electron beam lithography and reactive ion etching and treated with our BGL-GZ-83 anti adhesion layer [30,31]). Figure 2 shows a photograph and an AFM image of the master that was used. It contains, in total, 16 $4 \times 4 \text{ mm}^2$ large fields with four different periodicities. The line and space dimensions are 600 nm/1800 nm, 400 nm/1200 nm, 300 nm/900 nm and 200 nm/600 nm.

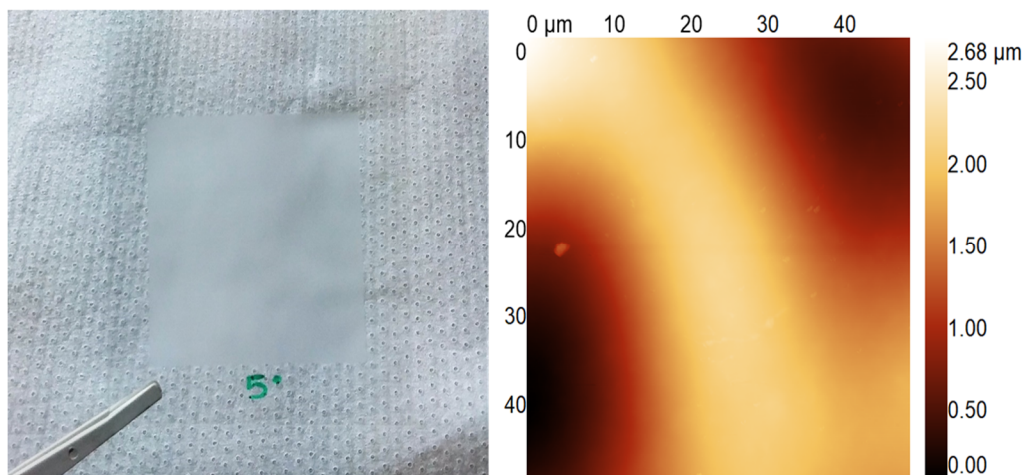


Figure 1. Left: photograph of the diffuser foil master. Right: AFM image of this master. The scan area is $50 \times 50 \mu\text{m}^2$.

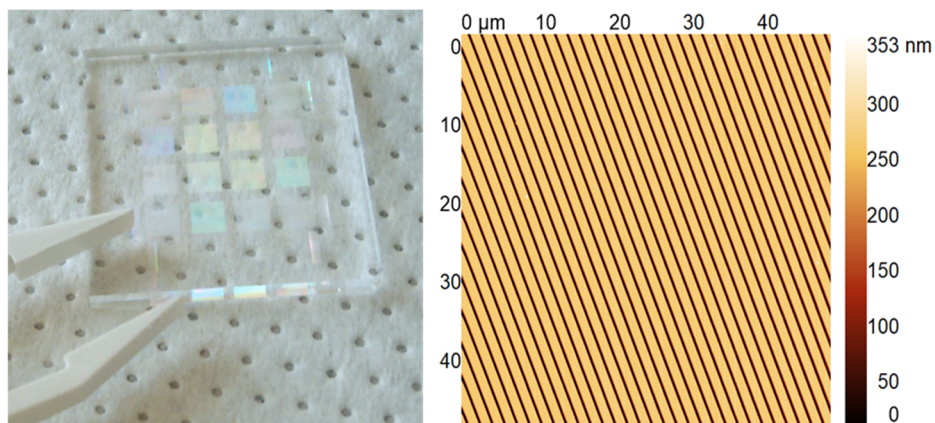


Figure 2. Left: photograph of the grating master. Right: AFM image of this master.

Again, OrmoComp was used for the final imprinting with the PDMS grating stamp. For the LTIL process, OrmoComp was diluted 1:2 with PGMEA (Propylene glycol monomethyl ether acetate) and then spin coated at 5,000 rpm on a silicon wafer. The solvent was then evaporated at $100\text{ }^{\circ}\text{C}$ on a hotplate for 1 min. Prior to spin-coating, the wafer was treated with Profactor's HMNP-12 adhesion promoter [32]. The PDMS stamp was carefully brought into contact with the coated wafer and then peeled off again. Then the stamp was used for UV-NIL on top of the diffuser substrate. Pressure was applied using a self-built air pressure-based imprinting setup, which allows very homogeneous pressure distribution even on curved substrates [33]. UV-curing was performed again using the high-power UV-LED system at 365 nm.

The whole process sequence is schematically sketched in Figure 3, beginning with the fabrication of the diffuser substrate (step A (diffuser stamp fabrication) and step B (nanoimprinting of OrmoComp on PVC)). Step C is the fabrication of the PDMS stamp from the grating master, which is then used in the LTIL process (D-H). First, the material transfer from the donor wafer to the stamp for reversal NIL is accomplished (steps D and E). The coated stamp is then brought in contact with the prestructured substrate (F, G). By applying external pressure, the flexible PDMS stamp conforms to the topography of the underlying substrate (G), the OrmoComp is cured (G) and the stamp is removed (H), finalizing the LTIL process. The sample now contains the hierarchical structures.

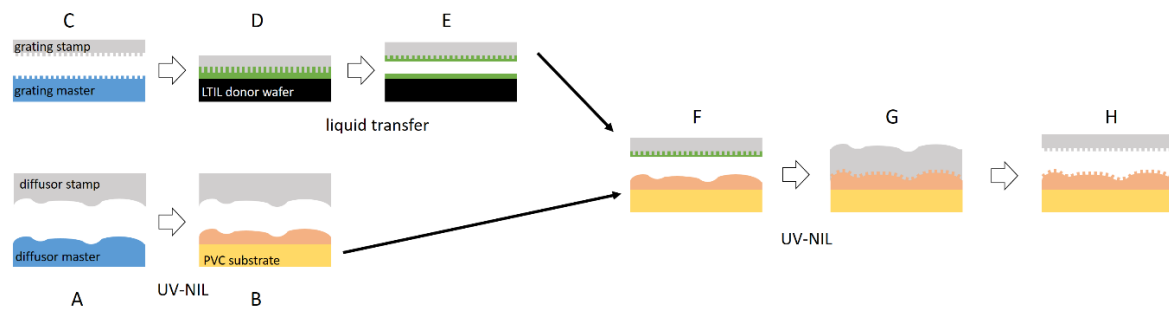


Figure 3. Process flow for master fabrication: First, a PDMS stamp from the diffuser master was fabricated (A), which is then used to imprint OrmoComp onto a PVC foil (B). Using a grating master, another PDMS stamp was made (C), which was used in an LTIL process (D,E) to print on the diffuser substrate (F–H). The flexible stamp conforms to the topography of the diffuser substrate as sketched in G. The results are the grating structures on top of the diffuser structures (H).

To avoid the trapping of air bubbles (especially in step G), two aspects are important. Firstly, the grating stamp has to be flexible enough to allow real conformal contact. In our case, the PDMS stamp was approximately 2 mm thick; for other substrate geometries thinner (i.e., more flexible) stamps will be necessary. Secondly, the contact geometry is critical. We bring the stamp into contact with one side of the substrate and then carefully lower the rest of the stamp in a lamination-type of process. Furthermore, nanoimprinting was performed in a vacuum [33]. Finally, the fact that PDMS is gas-permeable to some extent also helps in avoiding air bubbles [34,35].

The imprinting process was performed in such a way as to obtain four different areas on a single sample: the unstructured area, the diffuser structure alone, the grating structure alone, and an area with the hierarchical structure of grating on top of the diffuser. This was achieved by aligning the stamp to the substrate in such a way that the overlap between the diffraction grating pattern and the diffuser pattern was only achieved in a small area of the substrate.

From a sample that was prepared as described above, it is now possible to replicate a stamp for further nanoimprinting. A PDMS copy was prepared using conventional Sylgard 184 PDMS (1:10 mixing ratio, 23 h at 40 °C in a laboratory oven) as described above.

This stamp now contains the hierarchical structures and can be used in a conventional single step nanoimprint process. The imprint was again performed using OrmoComp as imprint material and a PVC foil as substrate. Figure 4 shows the processing sequence. In steps A–C the hierarchical structures sample is used as a master for working stamp fabrication. This working stamp is then used in a conventional Nanoimprint process (D–E). The advantage is that now the hierarchical structures can be replicated in a single nanoimprinting step.

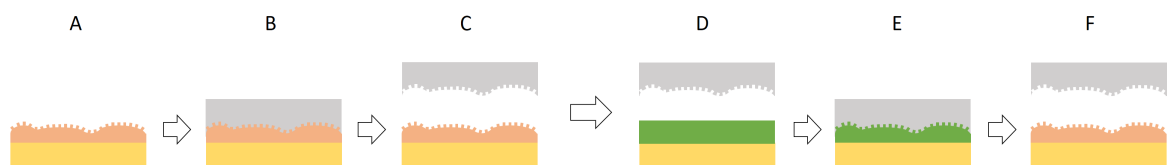


Figure 4. Process flow for stamp fabrication (A–C) and single step nanoimprinting of hierarchical structures (D–F).

3. Results

3.1. Hierarchical Stamp Master

Figures 4–8 show the result of these experiments. Figure 4 shows an optical micrograph image of the stamp master fabricated by combining conventional UV-NIL and LTIL. Both the diffuser structures and the grating structure can clearly be seen. AFM images from different positions of the same sample

are shown in Figure 5. The grating structure follows the topography of the underlying diffusor structure in a conformal way and is present both in the valleys and on the hills. Looking at the line scan from one of the AFM images (Figure 6), it can be seen that the height of both types of structures is preserved.

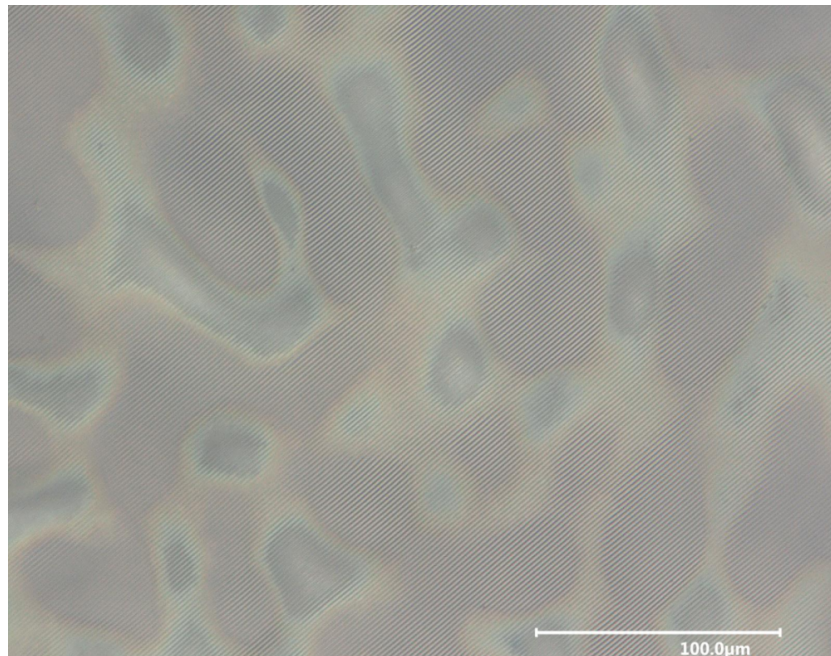


Figure 5. Optical micrograph of the grating on top of the diffusor structure. The lines and spaces follow the topography of the surface.

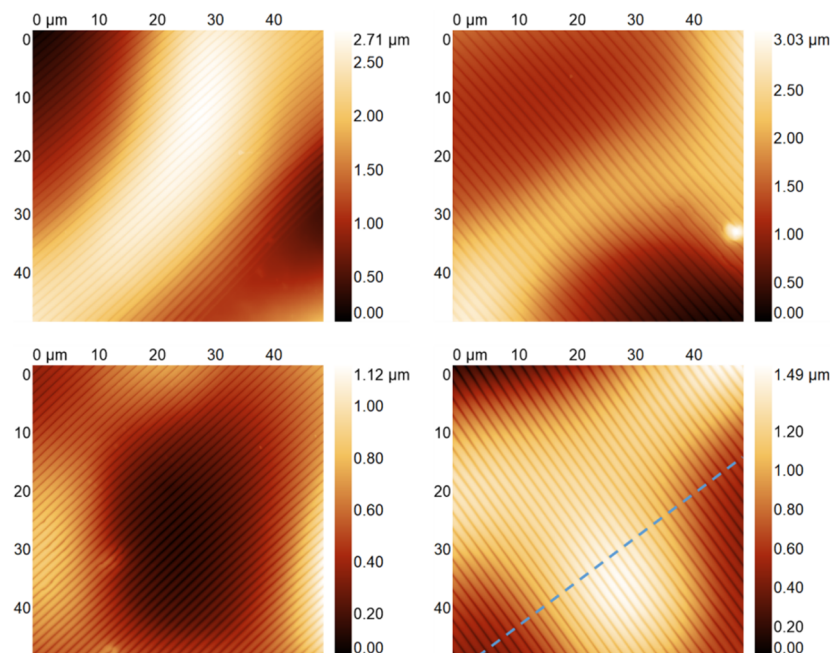


Figure 6. AFM images of the hierarchical structures master used for further imprinting. The left and right images have line and space dimensions of 300 nm/900 nm and 400 nm/1200 nm, respectively.

The dashed line in the lower right corner indicates the location of the extracted linescan shown in Figure 7.

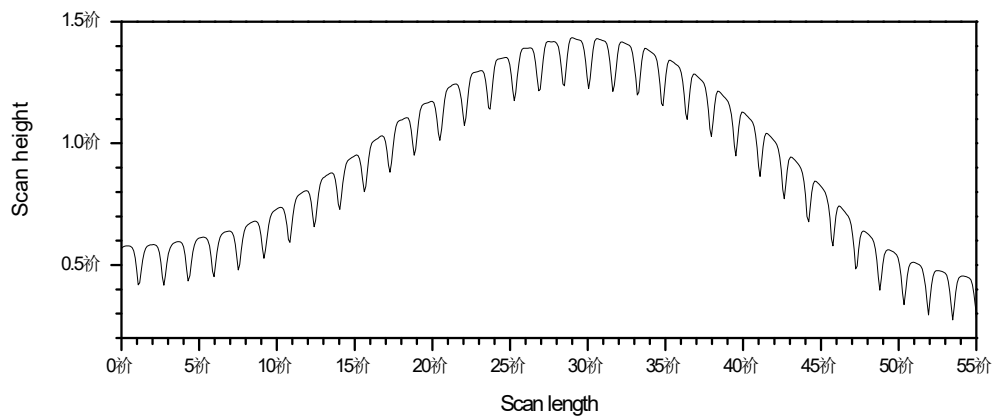


Figure 7. Line scan of the hierarchical structures master shown in Figures 5 and 6 above. The height of both types of structures is well preserved from the individual masters to the hierarchical structure.

Figure 8 compares the optical effects of the four different areas on the sample using a standard green laserpointer ($\lambda = 532$ nm). It can be seen that in the area with the hierarchical structures, both effects—the one of the diffusor and the one of the grating—are present.

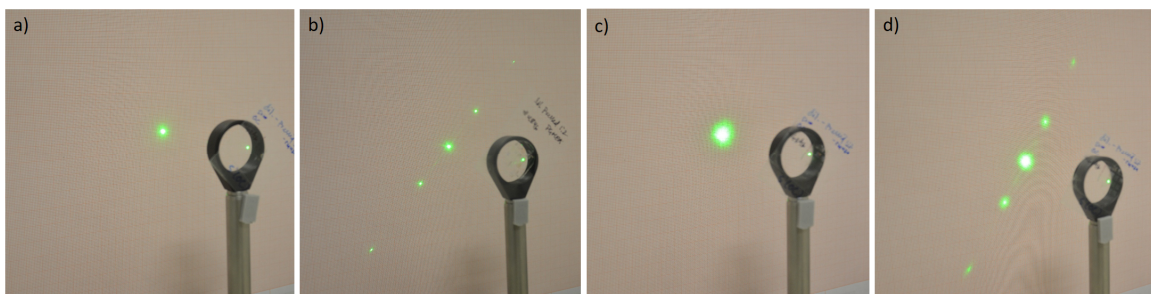


Figure 8. Photographs illustrating the optical effect of the differently structured areas by passing a green laser beam through the sample in 4 different areas: (a) unstructured, (b) only grating, (c) only diffusor and (d) grating on top of diffusor. The difference between b and d can be clearly seen.

3.2. Direct Hierarchical Nanoimprint

Figure 9 shows a compilation of four AFM images of the final sample, which was fabricated by a single imprint with a stamp copied from the hierarchical master sample. Due to the irregular structure of the diffusor, it was not possible to perform the measurements on the exact same spots as for the master again. However, our results show that the single step nanoimprint replication of hierarchical structures could be achieved with high fidelity. The line scan in Figure 10 shows the same characteristics as that produced by the flat grating master, the intermediate hierarchical structure master, and here on the final imprint. By evaluating the peak positions of the Fourier transformed images in Gwyddion [36], it was verified that the periodicities ($1.60 \mu\text{m}$ or $1.20 \mu\text{m}$, respectively) of the regions used for the line scans are identical on the grating master, the hierarchical structures master, and on the final imprint within the measurement error (± 60 nm, evaluated from 10 independent measurements using the 2D FFT function in Gwyddion). The volume shrinkage of the material, which is around 5%-7% according to the datasheet, does not play a significant role here, since the material is a thin layer fixed to a rigid, much thicker substrate. Shrinkage therefore will mainly happen in z-direction, since x- and y-directions are fixed. Due to the irregular nature of the diffusor structure, this effect could not be observed.

As far as the lifetime of the PDMS stamp is concerned, it strongly depends on the imprint resin used [34,37–40]. Furthermore, there are different types of PDMS that can be used, which also have different mechanical properties, e.g., h-PDMS [41,42] or X-PDMS [43].

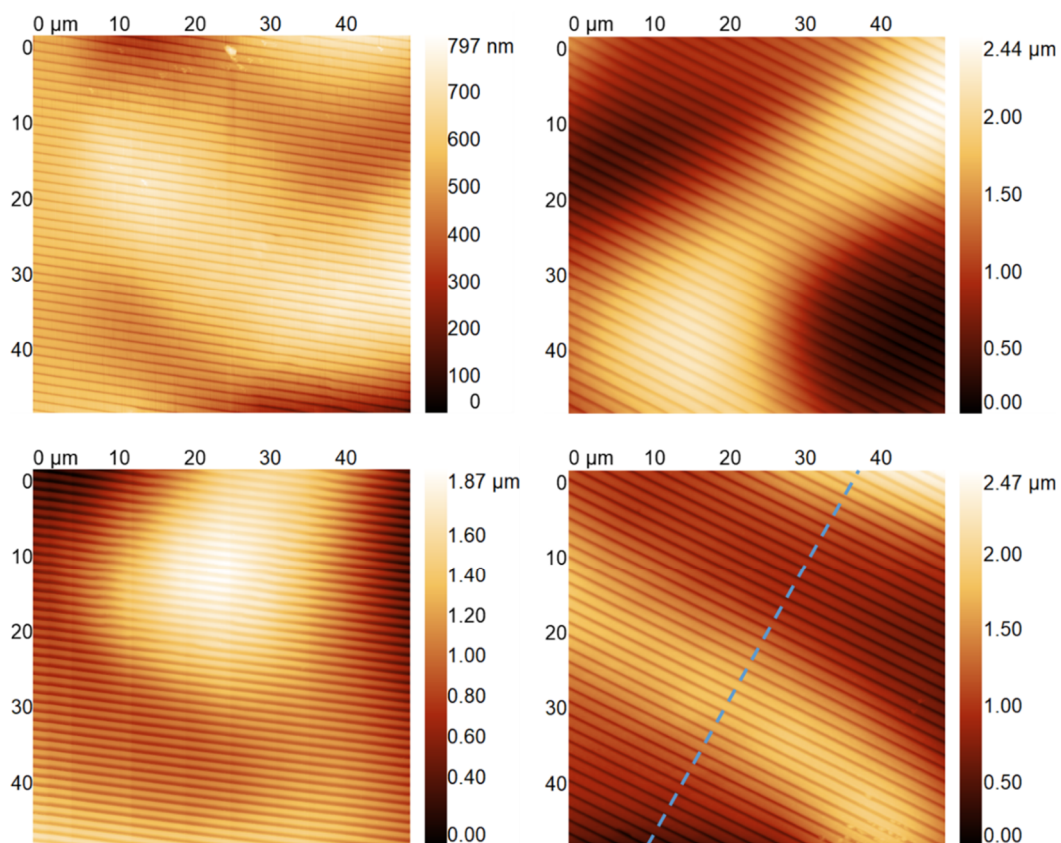


Figure 9. AFM image of the final imprint. The left and right images have line and space dimensions of 300 nm/900 nm and 400 nm/1200 nm, respectively. Comparing these with the results from Figure 5, it can be seen that the hierarchical structures could be replicated with high fidelity. The dashed line in the lower right corner indicates the location of the linescan shown in Figure 10.

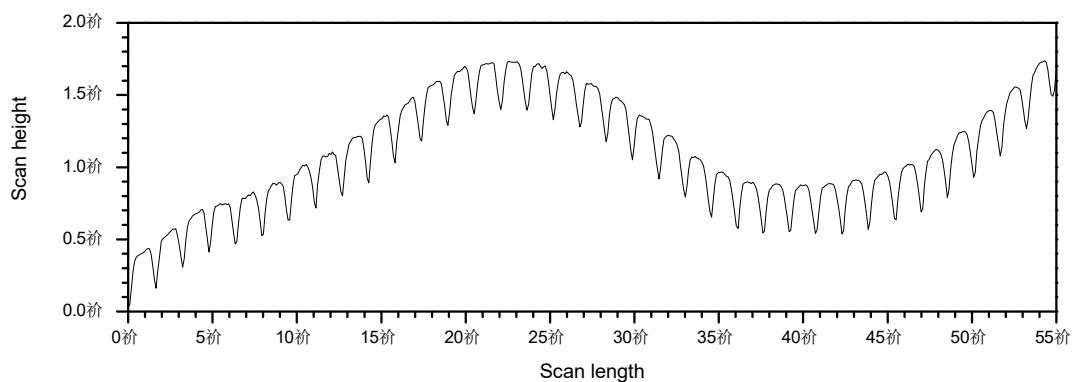


Figure 10. AFM linescan taken on the final imprint. The location is indicated by the dashed line in the lower right AFM image in Figure 9. Again, the height of both types of structures is well preserved from the individual masters to this final imprint.

4. Discussion

We showed that combining conventional NIL and LTIL is a suitable way to achieve multifunctional hierarchical surfaces. This has already been shown in other studies [26–28] and involves two separate nanoimprint steps and an unconventional nanoimprint method (LTIL). Using such a sample with a complex hierarchical geometry as a master for further stamp fabrication has several advantages in our opinion. To produce the final sample, the number of nanoimprint steps is reduced. Just one

imprinting step is necessary instead of two, and consequently, the overall number of process steps is significantly reduced - typically by a factor of two - reducing cost of the overall process significantly. Material use is also optimized, since a spin-coating step can be omitted, resulting in a greener and more cost-effective process. Furthermore, potential adhesion problems between the two layers (diffusor layer and grating layer) can be avoided, although we have seen no evidence that this might be a problem with the materials we used in our experiments.

As an example, we demonstrated the combination of diffraction grating and diffusor structure. Such a sample was also successfully used as a master to fabricate a working stamp for nanoimprint lithography to replicate hierarchical structures in a single process step. The choice of structures for this work was based on the availability of masters and the possibility to easily distinguish between the optical effects of the two. In general, we are optimistic that the same process can also be used for combinations of other structures and also for other types of effects, ranging from antimicrobial to superhydrophobic. Moreover, applications like antireflective moth-eye structures on micro lenses should be feasible with this process. We have seen in different processes that PDMS stamps are capable of strong deformations, while still maintaining conformal contact. Examples are given in Appendix A.

Another interesting aspect of the use of such a master structure is that—assuming vertical sidewalls in the master and stamp for the grating—the hierarchical master should have negative sidewalls in many areas on one side of the grating structures. We have seen no evidence that the presence of such undercut features represents a problem for the soft PDMS stamp that we used. Both for larger and smaller structures, it has been shown that PDMS or other types of soft stamp materials are capable of replicating such features [44,45]. We will continue to work on combining different types of structures.

Furthermore, we will also work to apply this process to larger areas (DIN A4 and more), to be able to implement such stamps in our roll-to-plate nanoimprint process.

In conclusion, we presented a nanoimprint-based process for the creation and cost-efficient replication of hierarchical surfaces, demonstrated using a diffusor and a diffraction pattern. Using two subsequent nanoimprint steps, we realized a master structure that was further used to replicate a stamp for nanoimprinting. With this stamp we were able to create the structure that was initially created by two separate nanoimprinting steps using one single step.

Author Contributions: Conceptualization, M.M.M.; investigation, A.R.M, H.M.A., T.M., M.J.H.; writing—original draft preparation, A.R.M.; writing—review and editing, M.M.M.; project administration, M.M.M.; funding acquisition, M.M.M. All authors have read and agreed to the published version of the manuscript.

Funding: This research was funded by the ANIIPF project (bmvit – Austrian Ministry for Transport, Innovation and Technology) as well as by the rollerNIL project (FFG - Austrian Research Promotion Agency grant number 843639) and the NEAT project (FFG - Austrian Research Promotion Agency grant number 871438).

Conflicts of Interest: The authors declare no conflict of interest.

Appendix A

To further illustrate the deformation properties for PDMS stamps, some examples are given here. The UV-NIL process used here was slightly different. The imprint material OrmoComp was droplet-dispensed, and the nanoimprinting was performed using a vacuum-based process with a tool described elsewhere in detail [33]. The substrate was generated using glass spheres glued to a glass substrate. Gluing was accomplished using a layer of OrmoComp. Due to the strong deformation of the PDMS stamp, the stamp stretches on top of the structures, as illustrated in Figures A1–A3. Figure A2 shows an additional SEM image of the sample shown in Figure A1. Figure A3 shows an optical micrograph of an additional sample.

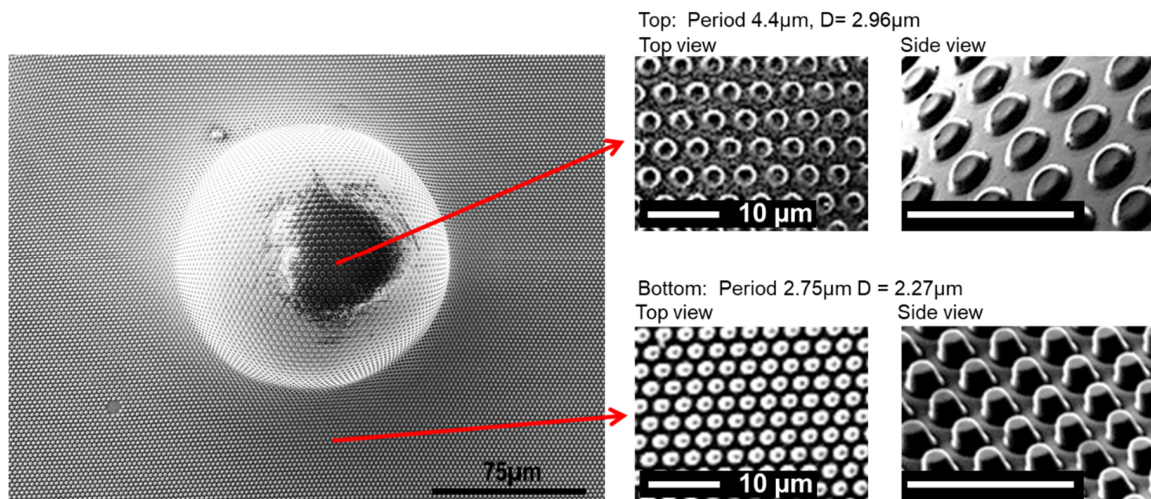


Figure A1. SEM images illustrating the deformation capabilities of PDMS stamps in nanoimprint lithography. The pattern on top of the sphere is significantly stretched. Consequently, the structures (pillars on the imprint, holes in the stamp) are also distorted. The period on the top is 160% of the period on the bottom, the diameter D of the features is also increased. The scale bars in the right images, which are cutouts from the left image and Figure A2, are $10\mu\text{m}$.

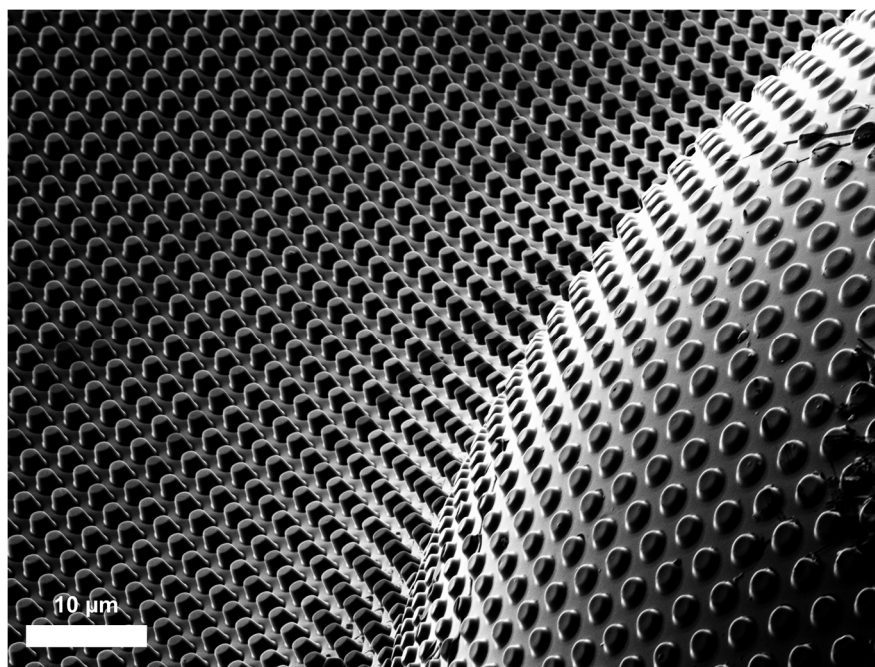


Figure A2. SEM image of microstructures nanoimprinted on top of a microsphere.

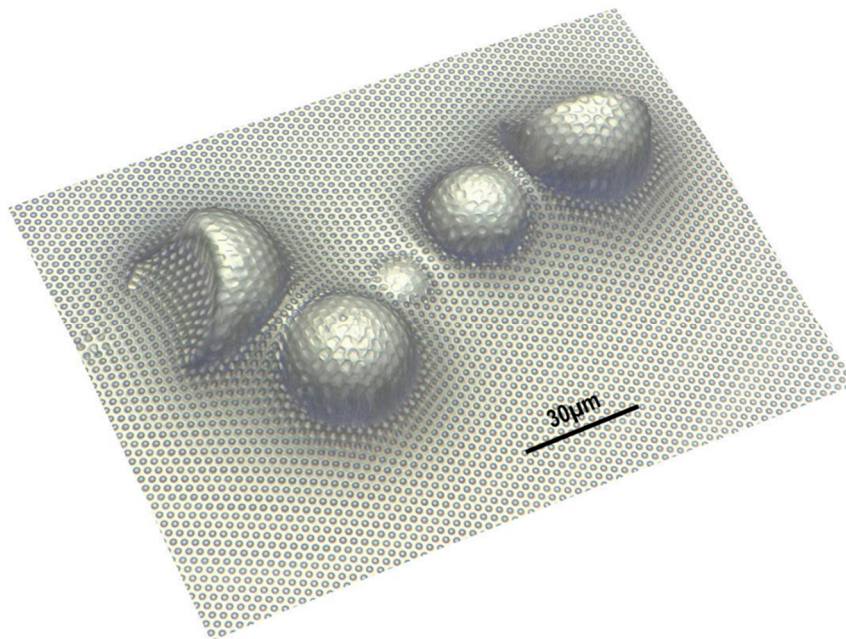


Figure A3. Optical micrograph (3D image stacking using a Keyence VHX-5000 digital microscope) of different types of microspheres over-imprinted with a PDMS stamp. In contrast to Figures A1 and A2 here, the stamp contained pillars instead of holes. It can clearly be seen that the pillars on the stamp are less stable under the imprinting pressure and collapse on top of the spheres, whereas the holes in the stamp remain more stable as can be seen in Figure A2.

References

1. Schiff, H. Nanoimprint lithography: An old story in modern times? *A review. J. Vac. Sci. Technol. B Microelectron. Nanometer Struct.* **2008**, *26*, 458. [[CrossRef](#)]
2. Haisma, J. Mold-assisted nanolithography: A process for reliable pattern replication. *J. Vac. Sci. Technol. B Microelectron. Nanometer Struct.* **1996**, *14*, 4124. [[CrossRef](#)]
3. Chen, Y.-P.; Lee, C.-H.; Wang, L.A. Fabrication and characterization of multi-scale microlens arrays with anti-reflection and diffusion properties. *Nanotechnology* **2011**, *22*, 215303. [[CrossRef](#)] [[PubMed](#)]
4. Xie, S.; Wan, X.; Yang, B.; Zhang, W.; Wei, X.; Zhuang, S. Design and Fabrication of Wafer-Level Microlens Array with Moth-Eye Antireflective Nanostructures. *Nanomaterials* **2019**, *9*, 747. [[CrossRef](#)] [[PubMed](#)]
5. Reboud, V.; Obieta, I.; Bilbao, L.; Saez-Martinez, V.; Brun, M.; Laulagnet, F.; Landis, S. Imprinted hydrogels for tunable hemispherical microlenses. *Microelectron. Eng.* **2013**, *111*, 189–192. [[CrossRef](#)]
6. Glinsner, T.; Kreindl, G.; Kast, M. Nanoimprint Lithography: The technology makes its mark on CMOS image sensors and in the nano-world. *Opt. Photonik* **2010**, *5*, 42–45. [[CrossRef](#)]
7. Kreindl, G.; Glinsner, T.; Miller, R.; Treiblmayr, D.; Födisch, R. High accuracy UV-nanoimprint lithography step-and-repeat master stamp fabrication for wafer level camera application. *J. Vac. Sci. Technol. B Nanotechnol. Microelectron. Mater. Process. Meas. Phenom.* **2010**, *28*, C6M57–C6M62. [[CrossRef](#)]
8. Gale, M. Replication techniques for diffractive optical elements. *Microelectron. Eng.* **1997**, *34*, 321–339. [[CrossRef](#)]
9. Gale, M.; Rossi, M.; Rudmann, H.; Saarinen, J.; Schnieper, M. Replicated diffractive optical elements in consumer products. In Proceedings of the Diffractive Optics and Micro-Optics, Rochester, NY, USA, 10–13 October 2004; OSA Publishing: Washington, DC, USA.
10. Osipov, V.; Doskolovich, L.L.; Bezus, E.A.; Drew, T.; Zhou, K.; Sawalha, K.; Swadener, G.; Wolffsohn, J.S.W. Application of nanoimprinting technique for fabrication of trifocal diffractive lens with sine-like radial profile. *J. Biomed. Opt.* **2015**, *20*, 025008. [[CrossRef](#)]
11. Schleunitz, A.; Schiff, H. Fabrication of 3D nanoimprint stamps with continuous reliefs using dose-modulated electron beam lithography and thermal reflow. *J. Micromech. Microeng.* **2010**, *20*, 095002. [[CrossRef](#)]

12. Gilles, S.; Meier, M.; Prömpers, M.; van der Hart, A.; Kügeler, C.; Offenhäusser, A.; Mayer, D. UV nanoimprint lithography with rigid polymer molds. *Microelectron. Eng.* **2009**, *86*, 661–664. [[CrossRef](#)]
13. Muehlberger, M.; Boehm, M.; Bergmair, I.; Chouiki, M.; Schoeftner, R.; Kreindl, G.; Kast, M.; Treiblmayr, D.; Glinsner, T.; Miller, R.; et al. Nanoimprint lithography from CHARPAN Tool exposed master stamps with 12.5nmhp. *Microelectron. Eng.* **2011**, *88*, 2070–2073. [[CrossRef](#)]
14. Junarsa, I.; Nealey, P.F. Fabrication of masters for nanoimprint, step and flash, and soft lithography using hydrogen silsesquioxane and x-ray lithography. *J. Vac. Sci. Technol. B Microelectron. Nanometer Struct.* **2004**, *22*, 2685. [[CrossRef](#)]
15. Zhang, X.; Huang, R.; Liu, K.; Kumar, A.S.; Shan, X. Rotating-tool diamond turning of Fresnel lenses on a roller mold for manufacturing of functional optical film. *Precis. Eng.* **2018**, *51*, 445–457. [[CrossRef](#)]
16. Mühlberger, M.; Rohn, M.; Danzberger, J.; Sonntag, E.; Rank, A.; Schumm, L.; Kirchner, R.; Forsich, C.; Gorb, S.; Einwögerer, B.; et al. UV-NIL fabricated bio-inspired inlays for injection molding to influence the friction behavior of ceramic surfaces. *Microelectron. Eng.* **2015**, *141*, 140–144. [[CrossRef](#)]
17. Neinhuis, C.; Barthlott, W. Characterization and distribution of water-repellent, self-cleaning plant surfaces. *Ann. Bot.* **1997**, *79*, 667–677. [[CrossRef](#)]
18. Autumn, K.; Liang, Y.A.; Hsieh, S.T.; Zesch, W.; Chan, W.P.; Kenny, T.W.; Fearing, R.; Full, R.J. Adhesive force of a single gecko foot-hair. *Nature* **2000**, *405*, 681. [[CrossRef](#)]
19. Gao, H.; Wang, X.; Yao, H.; Gorb, S.; Arzt, E. Mechanics of hierarchical adhesion structures of geckos. *Mech. Mater.* **2005**, *37*, 275–285. [[CrossRef](#)]
20. Taillaert, D.; Bienstman, P.; Baets, R. Compact efficient broadband grating coupler for silicon-on-insulator waveguides. *Opt. Lett.* **2004**, *29*, 2749–2751. [[CrossRef](#)]
21. Daubinger, R. Hierarchical Nanostructures for Energy Devices. *Johns. Matthey Technol. Rev.* **2016**, *60*, 151–157. [[CrossRef](#)]
22. Li, W.-D.; Ding, F.; Hu, J.; Chou, S.Y. Three-dimensional cavity nanoantenna coupled plasmonic nanodots for ultrahigh and uniform surface-enhanced Raman scattering over large area. *Opt. Express* **2011**, *19*, 3925–3936. [[CrossRef](#)] [[PubMed](#)]
23. Micro Resist Technology GmbH | Hybrid Polymers. Available online: <https://www.microresist.de/en/products/hybrid-polymers> (accessed on 27 February 2020).
24. Huang, X.D.; Bao, L.-R.; Cheng, X.; Guo, L.J.; Pang, S.W.; Yee, A.F. Reversal imprinting by transferring polymer from mold to substrate. *J. Vac. Sci. Technol. B Microelectron. Nanometer Struct.* **2002**, *20*, 2872. [[CrossRef](#)]
25. Koo, N.; Wuk Kim, J.; Otto, M.; Moormann, C.; Kurz, H. Liquid transfer imprint lithography: A new route to residual layer thickness control. *J. Vac. Sci. Technol. B Microelectron. Nanometer Struct.* **2011**, *29*, 06FC12. [[CrossRef](#)]
26. Moormann, C.; Koo, N.; Kim, J.; Plachetka, U.; Schlachter, F.; Nowak, C. Liquid transfer nanoimprint replication on non-flat surfaces for optical applications. *Microelectron. Eng.* **2012**, *100*, 28–32. [[CrossRef](#)]
27. Lee, J.; Park, H.-H.; Choi, K.-B.; Kim, G.; Lim, H. Fabrication of hybrid structures using UV roll-typed liquid transfer imprint lithography for large areas. *Microelectron. Eng.* **2014**, *127*, 72–76. [[CrossRef](#)]
28. Uchida, T.; Yu, F.; Nihei, M.; Taniguchi, J. Fabrication of antireflection structures on the surface of optical lenses by using a liquid transfer imprint technique. *Microelectron. Eng.* **2016**, *153*, 43–47. [[CrossRef](#)]
29. OrmoComp® | Micro Resist Technology GmbH. Available online: <http://www.microresist.de/en/products/hybrid-polymers/uv-imprint-uv-moulding/ormocomp%C2%AE> (accessed on 9 October 2017).
30. Mühlberger, M.; Bergmair, I.; Klukowska, A.; Kolander, A.; Leichtfried, H.; Platzgummer, E.; Loeschner, H.; Ebm, C.; Grützner, G.; Schöftner, R. UV-NIL with working stamps made from Ormostamp. *Microelectron. Eng.* **2009**, *86*, 691–693. [[CrossRef](#)]
31. Beschichtungen BGL-GZ-83 | PROFACOR. Available online: <https://www.profactor.at/loesungen/beschichtungen/> (accessed on 27 February 2020).
32. Beschichtungen HMNP-12 | PROFACOR. Available online: <https://www.profactor.at/loesungen/beschichtungen/> (accessed on 27 February 2020).
33. Köpplmayr, T.; Häusler, L.; Bergmair, I.; Mühlberger, M. Nanoimprint Lithography on curved surfaces prepared by fused deposition modelling. *Surf. Topogr. Metrol. Prop.* **2015**, *3*, 024003. [[CrossRef](#)]
34. Toepke, M.W.; Beebe, D.J. PDMS absorption of small molecules and consequences in microfluidic applications. *Lab. Chip* **2006**, *6*, 1484. [[CrossRef](#)] [[PubMed](#)]

35. Lamberti, A.; Marasso, S.L.; Cocuzza, M. PDMS membranes with tunable gas permeability for microfluidic applications. *RSC Adv.* **2012**, *106*, 61415–61419. [[CrossRef](#)]
36. Nečas, D.; Klapetek, P. Gwyddion: An open-source software for SPM data analysis. *Open Phys.* **2012**, *10*, 181–188. [[CrossRef](#)]
37. Haslinger, M.J.; Verschuuren, M.A.; van Brakel, R.; Danzberger, J.; Bergmair, I.; Mühlberger, M. Stamp degradation for high volume UV enhanced substrate conformal imprint lithography (UV-SCIL). *Microelectron. Eng.* **2016**, *153*, 66–70. [[CrossRef](#)]
38. Haslinger, M.J.; Mitteramskogler, T.; Kopp, S.; Leichtfried, H.; Messerschmidt, M.; Thesen, M.W.; Mühlberger, M. Development of a Soft UV-NIL Step&Repeat and Lift-Off Process Chain for High Speed Metal Nanomesh Fabrication. *Nanotechnology* **2020**, (in press).
39. Schmitt, H.; Duempelmann, P.; Fader, R.; Rommel, M.; Bauer, A.J.; Frey, L.; Brehm, M.; Kraft, A. Life time evaluation of PDMS stamps for UV-enhanced substrate conformal imprint lithography. *Microelectron. Eng.* **2012**, *98*, 275–278. [[CrossRef](#)]
40. Tucher, N.; Höhn, O.; Hauser, H.; Müller, C.; Bläsi, B. Characterizing the degradation of PDMS stamps in nanoimprint lithography. *Microelectron. Eng.* **2017**, *180*, 40–44. [[CrossRef](#)]
41. Schmid, H.; Michel, B. Siloxane Polymers for High-Resolution, High-Accuracy Soft Lithography. *Macromolecules* **2000**, *33*, 3042–3049. [[CrossRef](#)]
42. Pei, L.; Balls, A.; Tippets, C.; Abbott, J.; Linford, M.R.; Hu, J.; Madan, A.; Allred, D.D.; Vanfleet, R.R.; Davis, R.C. Polymer molded templates for nanostructured amorphous silicon photovoltaics. *J. Vac. Sci. Technol. Vac. Surf. Films* **2011**, *29*, 021017. [[CrossRef](#)]
43. Verschuuren, M.A. Substrate Conformal Imprint Lithography for Nanophotonics. Ph.D. Thesis, Utrecht University, Utrecht, The Netherlands, 2010.
44. Möllenbeck, S.; Bogdanski, N.; Scheer, H.-C.; Zajadacz, J.; Zimmer, K. Moulding of arrowhead structures. *Microelectron. Eng.* **2009**, *86*, 608–610. [[CrossRef](#)]
45. Muehlberger, M. More than Just 2D: Nanoimprinting and Complex Geometries. In Proceedings of the 32nd International Microprocesses and Nanotechnology Conference (MNC 2019), Hiroshima, Japan, 28–31 October 2019.



© 2020 by the authors. Licensee MDPI, Basel, Switzerland. This article is an open access article distributed under the terms and conditions of the Creative Commons Attribution (CC BY) license (<http://creativecommons.org/licenses/by/4.0/>).